

# Numerical Analysis of Melting/Solidification Problems using OpenFOAM

Erol Bicer<sup>a,b\*</sup>, Youngjae Park<sup>a</sup>, Youcho Choi<sup>a</sup>, Soon-Joon Hong<sup>a</sup>

<sup>a</sup>FNC Tech., Heungdeok IT Valley, Heungdeok 1-ro, Giheung-gu, Yongin-si, Gyeonggi-do, 446-908, Korea

<sup>b</sup>Department of Nuclear Engineering, Seoul National Univ., 1 Gwanak-ro, Gwanak-gu, Seoul 08826

\*Corresponding author: ebicer@fnctech.com

## 1. Introduction

Melting and solidification (Stefan-like) phenomena are crucial in various fields, including energy storage, materials science, and industrial processes like the fuel salt drain tanks of molten salt nuclear reactors. Understanding melting/solidification (hereinafter M/S) is paramount for optimizing design, efficiency, and safety in such applications. Phase Change Materials (PCMs) used in these processes span a diverse range, from pure metals and alloys to organic compounds and salt mixtures.

Problems related to M/S entail the numerical analysis of phase change phenomena, encompassing both isothermal and non-isothermal processes. Isothermal processes involve phase transitions occurring at constant temperatures, typically for pure materials, while non-isothermal phase changes occur over a range of temperatures, e.g., binary alloys.

Numerical simulations of M/S using Computational Fluid Dynamics (CFD) encounter a major challenge in tracking the moving interface between the solid and liquid phases. To overcome this obstacle, moving boundary [1] or enthalpy [2] methods are generally used.

The objective of this paper is to provide an introduction to the commonly adopted enthalpy methodology of M/S simulations in CFD using OpenFOAM and to demonstrate a benchmark experiment.

## 2. Methodology and Results

The literature review presented in Table I shows that the enthalpy method is more commonly used than the moving boundary method. This may be because implementing the enthalpy method is easier [3], as it involves additional source terms for momentum and energy equations, and there is no need to explicitly track the solidification front which requires solving two different energy equations for solid and liquid phases separately.

Table I: Recent M/S Studies

Reference	PCM	Phase Change	Interface Tracking
2017	Lopez	Pure Gallium	Isothermal Melting
2017	Hummel	Octadecane	Isothermal Melting
2018	Rad	Virtual	Isothermal Solidification
2018	Yamamoto et al.	Pure Gallium Pure Aluminium	Isothermal Melting Isothermal Solidification
2019	Faden et al.	Virtual Octadecane	Isothermal Solidification Isothermal Melting
2019	Singh et al.	Pure Tin	Isothermal Solidification
2020	Bouhal et al.	Pure Gallium	Isothermal Melting
2021	Tomita et al.	Paraffin	Melting and Freezing

### 2.1 Enthalpy-Porosity Technique

The enthalpy methods mentioned earlier incorporate latent heat ( $\Delta H$ ) considerations into the energy equation by assigning a latent heat value to each computational cell based on its temperature,  $\Delta H = f(T)$ . This adjustment reflects the absorption or release of latent heat during phase changes, acting as a heat source or sink in the energy equation. However, a key challenge arises in this approach which is the zero velocity condition when transitioning from liquid to solid phases. Voller et al. [2] explored different techniques to manage the zero solid velocity conditions and proposed a porosity approach. In this method, computational cells are treated as pseudo-porous media, with porosity adjusting between 1 (indicating a fully liquid cell) and 0 (representing a fully solid cell). Therefore, the technique is referred to as the enthalpy-porosity technique. Moreover, in addition to conduction, natural convection must also be taken into account as a relevant heat transfer mechanism. To account for the latent heat, porosity, and natural convection effects, appropriate volume source terms for the governing equations must be introduced as given in Eq. (1).

$$\begin{aligned} \nabla \cdot \vec{u} &= 0 \\ \frac{\partial \vec{u}}{\partial t} + \nabla \cdot (\vec{u}\vec{u}) &= -\nabla p_m + \nu \nabla^2 \vec{u} + \vec{S}_b + \vec{S}_u \quad (1) \\ \frac{\partial c_p T}{\partial t} + \vec{u} \cdot \nabla (c_p T) &= \nabla \cdot \left( \frac{\kappa}{\rho} \nabla T \right) + S_h \end{aligned}$$

### 2.2 Source Terms

Considering only the isothermal phase change (i.e. pure materials), the  $S_h$  term in Eq. (1) which accounts for the evolution of latent heat in the energy equation can be written as in Eq. (2). The temperature-dependent latent heat content can be given as the step function in Eq. (3) where  $T_m$  is the constant melting temperature and  $L$  is the latent heat of fusion. It should be noted that for non-isothermal cases, the mushy region can be modeled by modifying Eq. (3) to account for the transition zone between the solid and liquid phases. The details can be found in [2] for non-isothermal phase change modeling.

$$S_h = \frac{\partial(\rho \Delta H)}{\partial t} \quad (2)$$

$$f(T) = \begin{cases} L & T > T_m \\ 0 & T < T_m \end{cases} \quad (3)$$

Regarding the conservation of momentum, two additional source terms are added as  $\vec{S}_b$  and  $\vec{S}_u$  in Eq. (1).  $\vec{S}_b$  introduces the Boussinesq approximation to account for the natural convection effects as given in Eq. (4) where  $\beta$  is the thermal expansion coefficient. The Boussinesq method assumes that change in density has the most dominant effect on gravity, neglecting inertia while considering buoyancy effects.

$$\vec{S}_b = -\vec{g}\beta(T - T_m) \quad (4)$$

Finally, the last source term is the momentum conservation equation,  $\vec{S}_u$  accounts for the porosity effects forcing the velocities in the solid region to go to zero using the Darcy Law [4].  $\vec{S}_u$  given in Eq. (5) is a function of porosity  $\lambda$  adopted by [2] to reduce the velocities zero in the cells where phase change occurred. Porosity can be calculated as the fraction of liquid present. If a cell is entirely liquid, then its porosity will be one. Therefore, according to Equation (5), the result will be zero. However, if a cell undergoes a phase change, the Darcy source term will become the dominant one in the momentum equation, thus causing the velocity field to become zero. C and q are model coefficients that account for the morphology of the mushy region and avoiding division by zero, respectively.

$$\vec{S}_u = -C \frac{(1 - \lambda)^2}{(\lambda^3 + q)} \cdot \vec{u} \quad (5)$$

### 2.3 Implementation in OpenFOAM

OpenFOAM is a collection of C++ libraries used for solving continuum mechanics problems through the Finite Volume Method (FVM). A case directory is required, containing 0, constant, and system folders, each with different contents like initial/boundary conditions, mesh and phase properties, solver and system settings. When dealing with numerical solutions for phase changes, the enthalpy-porosity technique expresses the energy equation in terms of sensible enthalpy and adds a volumetric source into the energy equation to account for latent heat transfer during solidification or melting. Additionally, the momentum equation requires extra source terms. In OpenFOAM, these source terms can be directly added to the governing equations through the *fvModels* framework, which is specified in the optional *constant/fvModels* dictionary. For isothermal phase change problems, the *solidificationMeltingSource* model can be used. This model takes into account the presence of the solid phase in the flow field as a momentum porosity contribution and the energy associated with the phase change is added as an enthalpy contribution [5]. Lines 304, 338, and 339 of *solidificationMeltingSource* implemented consistent source terms for Eqs. (3), (4), and (5) respectively, according to Listing I and II.

```
297 void Foam::fv::solidificationMeltingSource::addSup
298 (
299     const volScalarField& rho,
300     fvMatrix<scalar>& eqn,
301     const word& fieldName
302 ) const
303 {
304     apply(rho, eqn);
305 }
```

Listing I: Implementation of Energy Source

```
331 forAll(cells, i)
332 {
333     const label celli = cells[i];
334
335     const scalar Vc = V[celli];
336     const scalar alpha1c = alpha1_[celli];
337
338     const scalar S = -Cu_*sqrt(1.0 - alpha1c)/(pow3(alpha1c) + q_);
339     const vector Sb = rhoRef_*g*beta_*deltaT_[i];
340
341     Sp[celli] += Vc*S;
342     Su[celli] += Vc*Sb;
343 }
```

Listing II: Implementation of Momentum Sources

### 2.4 Melting of Pure Gallium

Gau and Viskanta [6] experimentally investigated the impact of natural convection on the movement of solid-liquid interfaces and heat transfer during the M/S of gallium on a vertical wall. The experiment involved investigating M/S phenomena within a controlled environment using a rectangular test cell. This cell had dimensions of 8.89 cm (height) x 6.35 cm (width), with copper plate end walls serving as both heat source and sink as shown in Fig. 1.

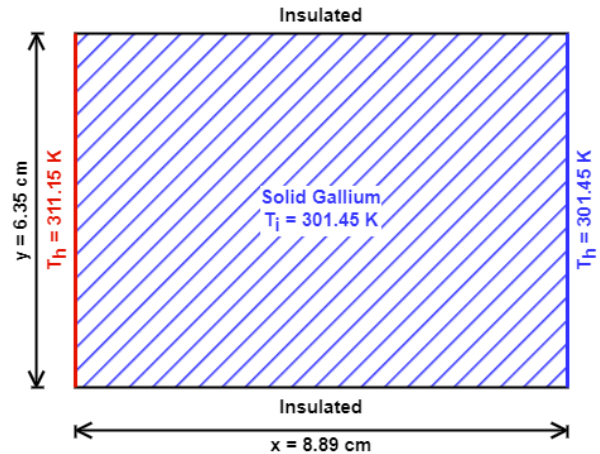


Fig. 1. Experimental Setup

The melting point of pure gallium is 302.93 K therefore initially the gallium is solid inside the domain. Once the experiment starts, the melting will be initiated and heat will dissipate into the system through a layer of molten gallium liquid. The thermophysical properties of pure gallium at 305.15 K used in this study were retrieved from [7] and shown in Table II.

Table II: Thermo-physical Properties of Pure Gallium

Liquid Density, $\rho$	$6093 \text{ kg} \cdot \text{m}^{-3}$
Reference Density, $\rho_{\text{ref}}$	$6095 \text{ kg} \cdot \text{m}^{-3}$
Reference temperature, $T_{\text{ref}}$	$29.78^\circ\text{C}$
Thermal Expansion Coefficient, $\beta$	$1.2 \times 10^{-4}$
Thermal Conductivity, $k$	$32.0 \text{ W} \cdot \text{m}^{-1} \cdot \text{K}^{-1}$
Latent Heat of Fusion, $L$	$80.16 \text{ kJ} \cdot \text{kg}^{-1}$
Specific Heat Capacity, $C$	$381.5 \text{ J} \cdot \text{kg}^{-1}$
Dynamic Viscosity, $\mu$	$1.81 \times 10^{-3} \text{ kg} \cdot \text{m}^{-1} \cdot \text{s}^{-1}$
Prandtl Number, $Pr$	$2.16 \times 10^{-2}$
Stefan Number, $Ste$	0.039
Rayleigh Number, $Ra$	$6 \times 10^5$

## 2.5 Simulation Setup

The domain shown in Fig. 1 is meshed into  $90 \times 63$  pure hexahedra cells, resulting in a square cell size of approximately 0.1 cm using the *blockMeshDict* utility of OpenFOAM V-11. The *fixedValue* boundary condition is applied to the left and right walls, which imposes a constant temperature value at the boundary. The *zeroGradient* boundary is used to simulate insulated walls at the top and bottom of the domain. A standard *kEpsilon* turbulence model is utilized to account for turbulence effects. As for the solver, the *fluid* solver module was used, which is a solver for steady or transient turbulent flow of compressible fluids with heat transfer using the flexible PIMPLE (PISO-SIMPLE) algorithm. The module allows the optional *fvModels*, in which the *solidificationMeltingSource* can be set up. The simulations are set to run for 1,200 seconds with adjustable time steps of a maximum of 0.25 Courant number.

## 2.6 Results

The Figs. (2) through (4) illustrate the time evolution of the melt front, temperature, and velocity at 120, 480, 900, and 1200 seconds, respectively. In Fig. 2, the position of the melt front demonstrates that it is planar after two minutes when natural circulation is about to begin. It can be seen that the upper section of the melt front moves faster than the lower section, which can be explained by examining the temperature and velocity profiles in Figs. (3) and (4), respectively, along with the melt front in Fig. (1). When the fluid is heated at the wall, it rises as it becomes less dense and carries thermal energy across the cavity. When the warm fluid reaches the solid front, it transfers heat and causes melting. The upper section of the solid front, where the warm fluid directly impacts, melts beyond the mean position of the front, resulting in a change in morphology. As time progresses, the natural convection effects increase and the melt front fully develops as the characteristic shape in Fig. 1. This process demonstrates how natural convection influences energy transport and morphology in the system. Therefore it can be concluded that the convection effects determine the shape of the melt front during M/S.

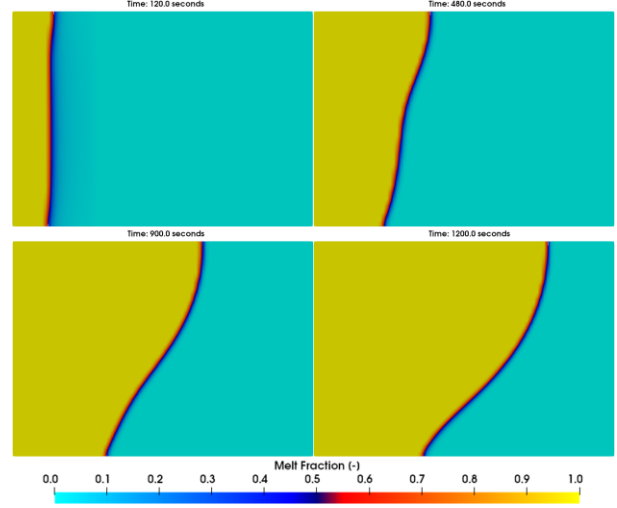


Fig. 2. Time Evolution of Melt Fraction Profile

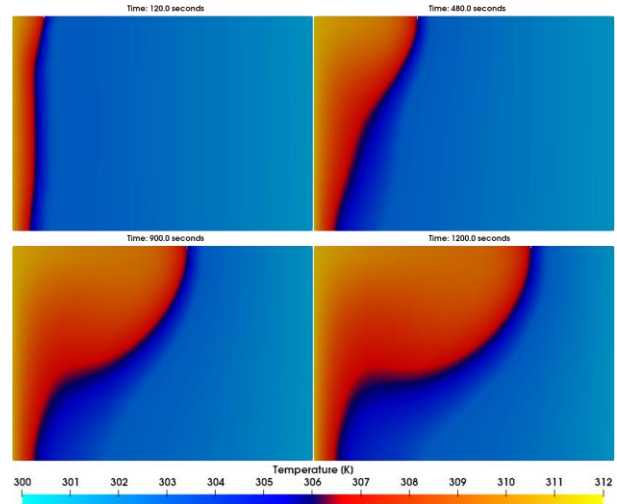


Fig. 3. Time Evolution of Temperature Profile

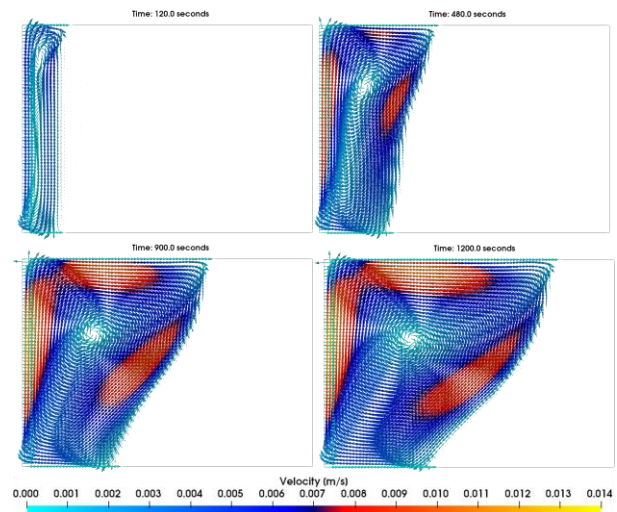


Fig. 4. Time Evolution of Velocity Profile

The melt fronts of the experiment [6] were compared with the OpenFOAM simulation results in Fig. 5 at various times. The simulation successfully captured the morphology of the melt front of the experiment at given times. However, there was a noticeable difference between the experiment and the simulation results at minute 17. At this point, the melt front in the experiment fell back behind the melt front line at minute 15, indicating solidification. However, this was not observed in the simulation, and there were no other heat sources or sinks to alter the evolution of the melt front. Therefore, this discrepancy could be the result of experimental errors such as ineffective insulation or measurement errors. Additionally, in a 2D simulation of melting/solidification problems, small discrepancies between computed and experimental results may arise due to several three-dimensional effects such as the missing thermal gradients and convection currents in the third dimension. These gradients and currents can affect heat transfer patterns and the distribution of heat and thus the position of the melt front.

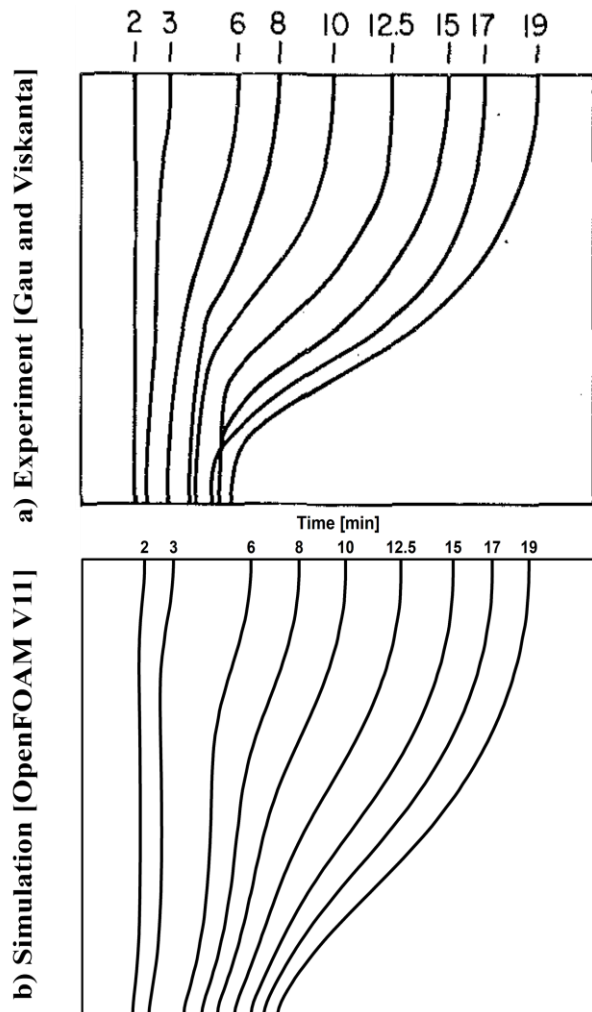


Fig. 5. Experiment and Simulation Melt Fronts

### 3. Conclusions

This study introduces the general concept of the isothermal M/S phenomenon and evaluates the capabilities of OpenFOAM, which utilizes an enthalpy-porosity technique to track the melting and/or solidification front using *solidificationMeltingSource*. This model introduces two sources into the momentum equation and one source into the energy equation. The capabilities of OpenFOAM were evaluated by using a gallium melting experiment from the literature.

It was found that OpenFOAM predicted the melt front position excellently. During the early stages of melting, the fluid motion is weak before the buoyancy effects take place. The shape of the melt front is nearly flat and parallel to the heated wall. The dominant heat transfer mechanism is conduction. However, as time goes on, the buoyancy-driven natural convection takes over, and the melt front proceeds faster in the upper section since the heated fluid rises.

The general discrepancies between the experiment and simulation results were attributed to the three-dimensional effects and possible measurement errors. Currently, OpenFOAM-V11 does not support the non-isothermal phase change, and therefore the mushy region of binary alloys cannot be simulated. As a future study, the implementation of non-isothermal phase change into OpenFOAM is planned.

### REFERENCES

- [1] E.M. Sparrow, S.V. Patankar, S. Ramadhyani, Analysis of Melting in the Presence of Natural Convection in the Melt Region, *Journal of Heat Transfer*. 99 (1977) 520–526. <https://doi.org/10.1115/1.3450736>.
- [2] V.R. Voller, C. Prakash, A Fixed Grid Numerical Modelling Methodology for Convection-diffusion Mushy Region phase-change Problems, *International Journal of Heat and Mass Transfer*. 30 (1987) 1709–1719. [https://doi.org/10.1016/0017-9310\(87\)90317-6](https://doi.org/10.1016/0017-9310(87)90317-6).
- [3] Mahdi Torabi Rad, *solidificationMeltingSource: a Built-in fvOption in OpenFOAM® for Simulating Isothermal Solidification*, in: J.M. Nóbrega, H. Jasak (Eds.), Springer EBooks, Springer Nature, 2019: pp. 455–464. [https://doi.org/10.1007/978-3-319-60846-4\\_32](https://doi.org/10.1007/978-3-319-60846-4_32).
- [4] P.C. Carman, *Fluid Flow through Granular Beds*, AICHE. 15 (1937).
- [5] OpenFOAM Foundation, *OpenFOAM | Free CFD Software | The OpenFOAM Foundation*, Openfoam.org. (n.d.). <https://openfoam.org/>.
- [6] C. Gau, R. Viskanta, Melting and Solidification of a Pure Metal on a Vertical Wall, *Journal of Heat Transfer*. 108 (1986) 174–181. <https://doi.org/10.1115/1.3246884>.
- [7] A.D. Brent, V.R. Voller, K.J. Reid, Enthalpy-Porosity Technique for Modeling Convection-Diffusion Phase Change: Application to the Melting of a Pure Metal, *Numerical Heat Transfer, Part B: Fundamentals*. 13 (1988) 297–318. <https://doi.org/10.1080/10407798808551388>.